



INITIATION CONDITIONS OF LIQUID ASCENT OF THE COUNTERCURRENT TWO-PHASE FLOW IN VERTICAL PIPES (IN THE PRESENCE OF TWO-PHASE MIXTURE IN THE LOWER PORTION)

Y. KOIZUMI and T. UEDA

Department of Mechanical Engineering, Kogakuin University, 2665-1, Nakano-machi, Hachioji-shi, Tokyo 192, Japan

(Received 5 January 1995; in revised form 27 June 1995)

Abstract—Experiments on the countercurrent two-phase flow of air and water were conducted using vertical pipes of 10–26 mm in diameter to investigate the initiation conditions of liquid ascent. When a liquid film flowed down to a bubbling two-phase mixture in the lower portion of the pipe, liquid ascent began at much lower gas velocities than usual flooding velocities without the bubbling two-phase mixture. In most cases, liquid ascent occurred in a slug flow state. The initiation conditions of the liquid ascent were analyzed physically by considering the level swell of the two-phase mixture fluctuating around the mean height.

Key Words: two-phase flow, countercurrent flow, two-phase mixture, slug flow, falling liquid film, liquid ascent, flooding

1. INTRODUCTION

The countercurrent two-phase flow in a vertical open pipe is normally of an annular type, where liquid flows down on the wall as a film. It has been known that increasing a gas flow rate flowing upwards in a core of the pipe, a point is reached where a part of the liquid begins to reverse in the upward direction. The phenomenon is commonly called flooding and often leads to the abrupt deterioration of efficiency in heat transfer equipment. It has been widely accepted that flooding is caused by interaction between the gas flow and large disturbances formed on the film (Ueda 1981).

However, when a two-phase mixture exists in the lower portion of a pipe and then gas and liquid flow countercurrently, liquid behavior seems to be different from that of the flooding encountered in the open systems described above. Such countercurrent two-phase flows are supposed to come out in a core or steam generator U-tube during loss-of-coolant accidents of nuclear reactors. This phenomenon is one of the important issues to be resolved for nuclear reactor safety assessment. Similar flow conditions are also observed in closed two-phase thermosiphons. It has been pointed out that the behavior of the two-phase mixture level is closely related to the performance limit of the thermosiphons (Ueda & Miyashita 1991).

Ueda & Koizumi (1993) examined the liquid behavior of the bubbling two-phase mixture in vertical pipes to which liquid was supplied as a falling film. The present study followed this and the initiation conditions of liquid ascent in such circumstances were investigated.

In this paper, flooding is defined, as is widely noted, as the initiation of liquid ascent in the countercurrent two-phase flow in a vertical pipe. Open and bottom-closed systems are used terminologically for the case where only a falling film and an ascending gas flow are present in the pipe and for the case where the liquid film flows down to the bubbling two-phase mixture in the lower portion of the pipe, respectively. Flooding velocities were examined experimentally for both open and bottom-closed systems using air and water at atmospheric pressure and room temperature. The results were analyzed physically based upon Ueda & Koizumi's study on the level swell of the bubbling two-phase mixture with the falling film.

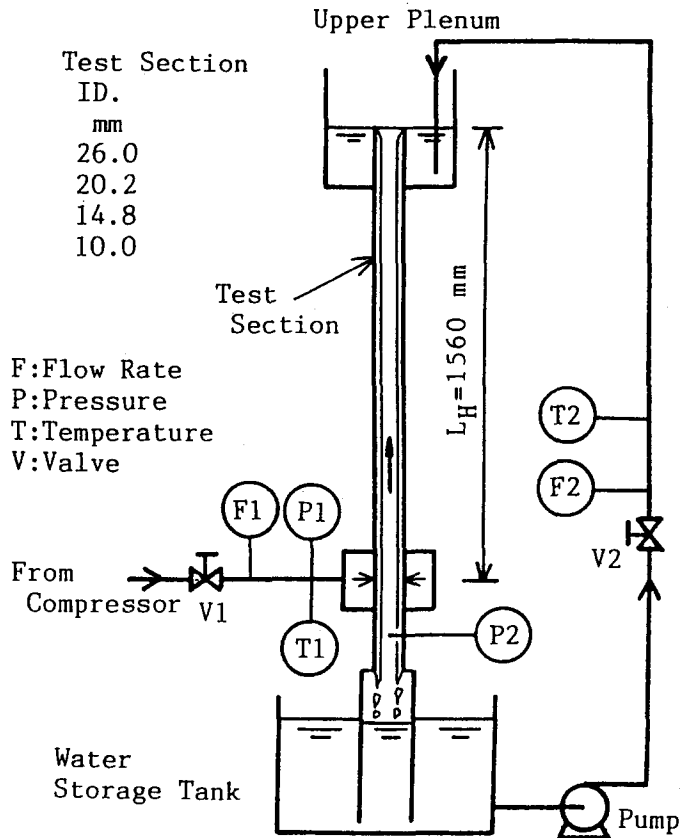


Figure 1. Schematic diagram of the experimental apparatus for open system flooding.

2. EXPERIMENTAL APPARATUS AND PROCEDURES

2.1. Open-system flooding experiments

The experimental apparatus used in the present study is schematically shown in figure 1. Air, supplied from a compressor through a rotameter, is injected into a test pipe through 12 nozzles of 1 mm diameter drilled circumferentially at the lower end of the test pipe. The outlet of the piping connecting to the bottom end of the test pipe is immersed in water in a storage tank so that the injected air may flow upwards. Water is pumped from the tank through a rotameter and into an upper plenum. Then, water flows down gravitationally on the inner surface of the test pipe in the form of a film and returns to the water storage tank beneath the test pipe.

Four Pyrex glass pipes were used for the test pipe. The inner diameters of these were $D = 10.0$, 14.8, 20.2 and 26.0 mm, respectively. The distance between the top end of the test pipe and the air inlet nozzles was 1560 mm. The top-end inner-edge of each test pipe was rounded off with a few millimetres radius in order that water may flow into the test pipe smoothly and uniformly.

Deionized water was used in the experiments. The rotameters were calibrated prior to the experiments.

While observing a flow state, the air flow rate was increased gradually in the step-wise fashion for a fixed water flow rate until water splashing-out from the top end of the test pipe was first perceived. The initiation of the water splashing-out was defined as the onset of liquid ascent, i.e. the open system flooding. Flow states were also recorded on a video recorder. The scope of the experiments was:

superficial velocity of air: $U_G = \sim 5$ m/s,

superficial velocity of falling water: $U_{fL} = 0.004 \sim 0.2$ m/s.

2.2. Bottom-closed system flooding experiments

The apparatus used is essentially the same as that used in the open system flooding experiments as shown in figure 2. The water storage tank is set up separately from the test pipe. A stand pipe of a 6 mm i.d. glass pipe is introduced for measuring the collapsed liquid level in the test pipe. For the test pipe of $D = 26.0$ mm, the diameter and the number of nozzles for air injection into the test pipe is increased to 2 mm and 18, respectively, to avoid excess pressure rise at the air flow meter. In a previous study (Ueda & Koizumi 1993), it was confirmed that the effects of size and the number of nozzles on the behavior of the bubbling two-phase mixture are little in the range of size from 0.75 to 2 mm and of numbers from 4 to 12 for the pipe of $D = 20.2$ mm.

The experimental procedure was similar to that of the open system flooding experiments. By adjusting a valve, V3, shown in figure 2 and balancing the water flow rate exiting from the bottom of the test pipe with a film flow rate U_{fL} , the water column height L_e in the stand pipe was maintained at a specified height. The air flow rate was increased gradually and stepwise for the fixed U_{fL} and L_e until water splashing-out from the top of the test pipe was perceived. Initiation of the water splashing-out was defined as the onset of liquid ascent, i.e. bottom-closed system flooding, as in the open system experiments.

The experiments were conducted in a range of U_G up to 5 m/s and U_{fL} from 0.004 to 0.12 m/s for the same four pipes that were used in the open system experiments. The collapsed water levels L_e tested were 60, 120, 240 and 360 mm.

3. EXPERIMENTAL RESULTS

3.1. Open system flooding experiments

Flooding velocities U_G obtained are plotted against the superficial velocities of the falling film U_{fL} in figure 3. The flooding velocities are defined here as the superficial velocities of air at the time when water splashing-out from the top end of the test pipe was initiated. In the figure, it is

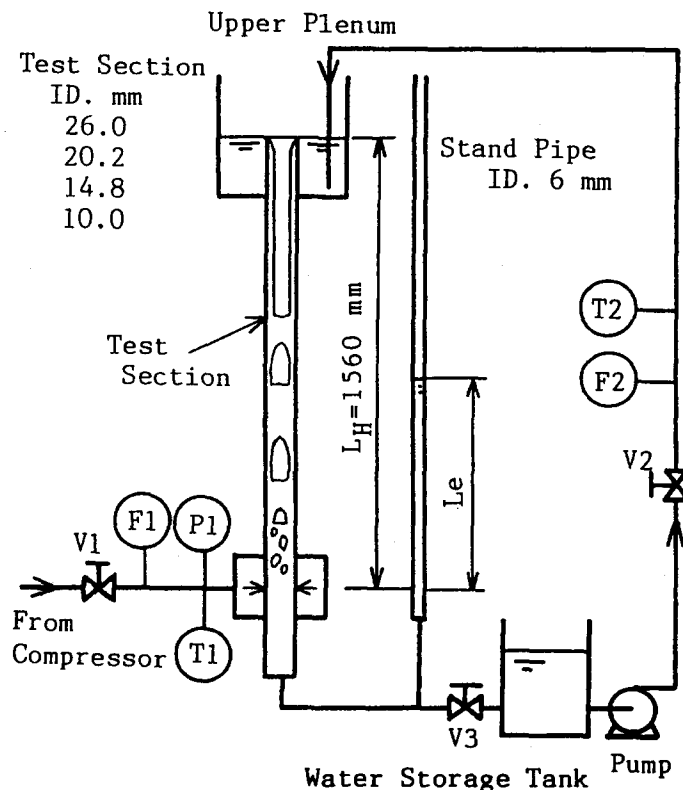


Figure 2. Schematic diagram of the experimental apparatus for bottom-closed system flooding.

recognized that the flooding velocities decrease with a decrease in diameter D and an increase in U_{fL} .

When U_{fL} was increased further, air bubbles of a plug type flowed downwards with water in the cases of $D = 10.0$ and 14.8 mm. In figure 3, points where U_{fL} is equal to the plug rising velocity in a stagnant liquid column (White & Beardmore 1962)

$$u_s = c_s \sqrt{gD} \tag{1}$$

are marked with dashed lines. The value of the coefficient c_s for such a low viscosity liquid as water is a function of $Eö = \rho_L g D^2 / \sigma$ and $Y = g \eta_L^4 / \rho_L \sigma^3$, and is equal to 0.35 for $Eö \geq 100$. Here g is the gravitational acceleration, η_L the liquid viscosity, ρ_L the liquid density and σ the surface tension. The actual values of c_s for $D = 26.0, 20.2, 14.8$ and 10.0 mm are 0.34, 0.33, 0.31 and 0.23, respectively, for the present experimental conditions. It is realized that when bubbles take the form of a plug and $U_{fL} > u_s$, the air plugs move down with the liquid and the stable flooding condition is no longer established.

Four curves are included in figure 3 representing values of U_G and U_{fL} calculated with the Suzuki & Ueda (1977) correlations for the flooding velocities. The correlations were derived for a system in which disturbances generated on the film by the entry effects of gas and liquid were suppressed as carefully as possible. The present experimental results show similar tendencies of the correlation values, however, they are considerably lower. It is common knowledge that the flooding velocities are considerably affected by the detailed geometry of the gas and the liquid entry and the way in which gas and liquid are introduced into a channel. When the disturbances or waves are easily built up on the liquid film, flooding occurs at the lower gas velocities. In the present experiments, since

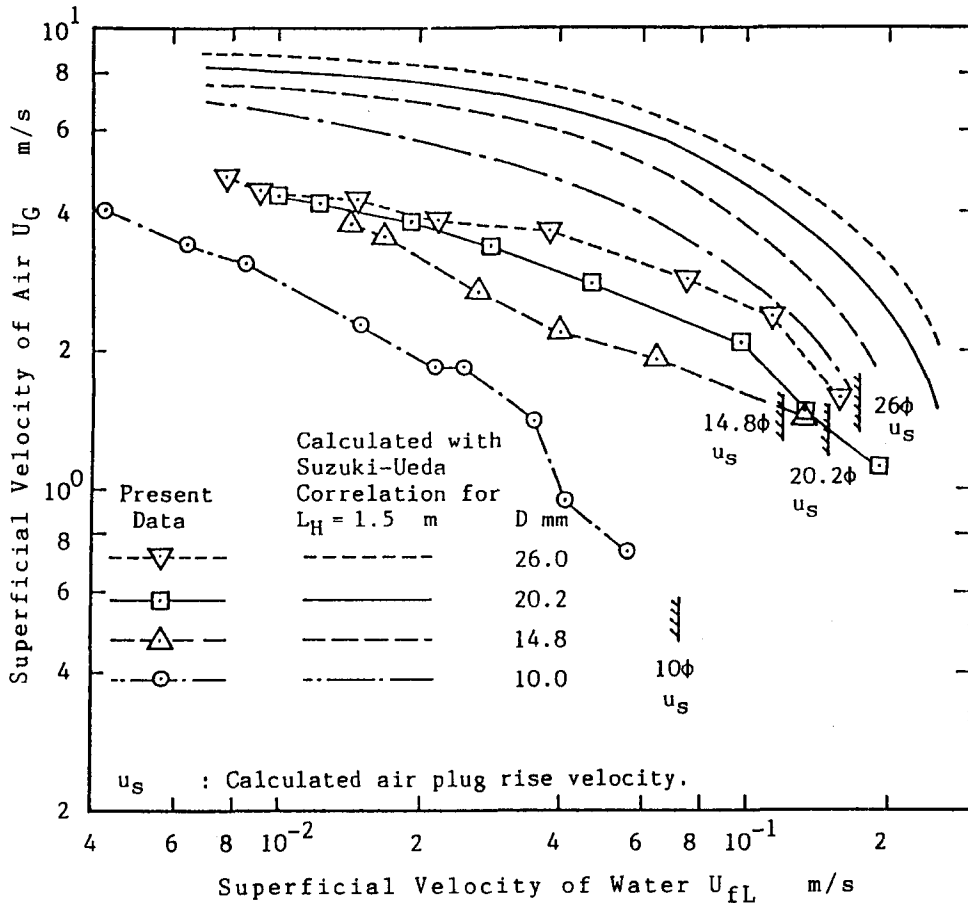


Figure 3. Flooding velocities of the open system.

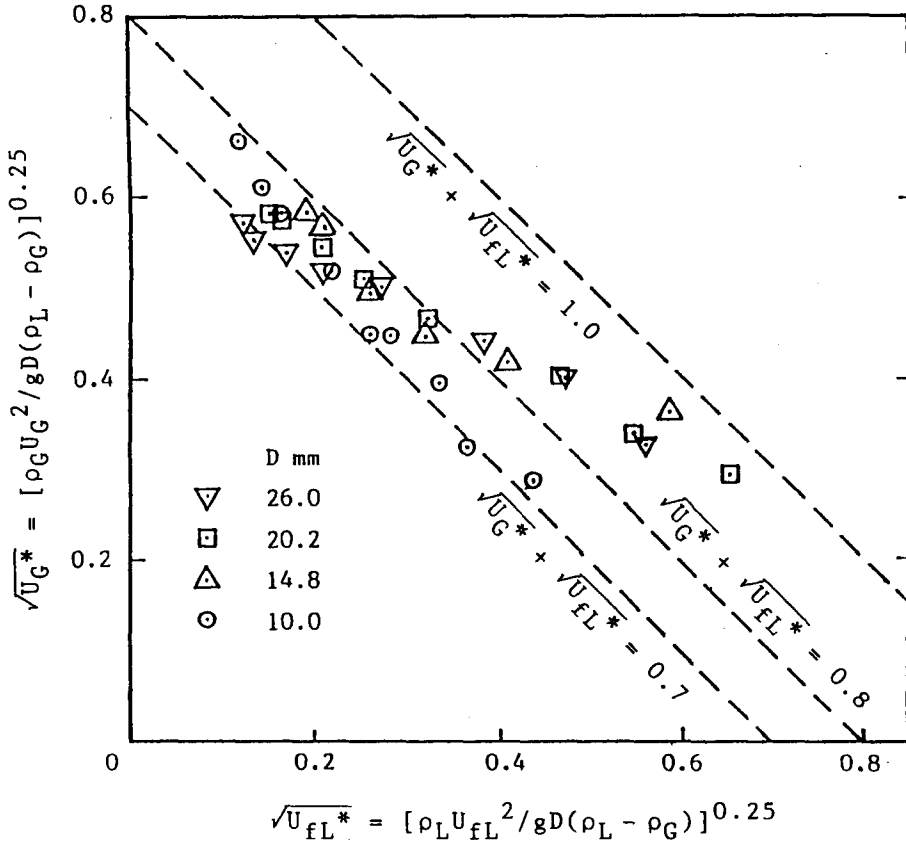


Figure 4. Flooding velocities of the open system; correlated results with the Wallis equation.

air was injected into the test pipe through small nozzles drilled in the pipe wall, it is supposed that the air flow had a higher level of turbulence, thus promoting disturbance growth on the liquid film.

The flooding velocities are presented in figure 4 in terms of non-dimensional volumetric fluxes of gas and liquid;

$$U_G^* = \frac{U_G}{\sqrt{gD}} \left(\frac{\rho_G}{\rho_L - \rho_G} \right)^{1/2}$$

and

$$U_{fL}^* = \frac{U_{fL}}{\sqrt{gD}} \left(\frac{\rho_L}{\rho_L - \rho_G} \right)^{1/2}$$

Here, subscripts G and L are for gas and liquid, respectively. The results are compared with the Wallis equation (Wallis 1969)

$$\sqrt{U_G^*} + \sqrt{U_{fL}^*} = C. \tag{2}$$

The constant C is normally in the range of 0.7–1.0 and takes lower values when gas and/or liquid are introduced by the method which tends to create larger disturbances on the film. The present data show that $C = 0.7–0.8$, except for a region of larger U_{fL} , suggesting that the liquid film was disturbed considerably.

In the case of larger U_{fL} (approximately $U_{fL}^* > 0.35$), the data plots show a different tendency from values calculated with [2]. In the region of $U_{fL}^* \leq 0.35$, the flow state immediately before the flooding initiation was of annular type. However, in the region of $U_{fL}^* > 0.35$, the flow state changed to a churn or slug type where the gas phase forms large bubbles or plugs with an irregular and unstable interface in the continuous liquid phase.

It is concluded that the open system flooding velocities of the present facility are well represented by [2] with $C = 0.7–0.8$. However, when the film flow rate increases and the flow state at the

flooding initiation turns from an annular type into a slug or a churn type, a different trend from [2] is pronounced; the decreasing rate of flooding velocity decreases with an increase in the film flow rate.

3.2. Bottom-closed system flooding experiments

Flooding velocities U_G of the bottom-closed system, obtained for $D = 26.0$ and 14.8 mm, are plotted against the superficial velocities of the falling film U_{fL} in figures 5 and 6, respectively. The results of the open system, noted as $L_e = 0.0$ mm, are also included in the figures for comparison. Dashed lines express the values calculated by [2].

In the case of $L_e = 60$ mm and $U_{fL} = 0.0045$ m/s in figures 5 and 6, the water splashing-out from the top of the test pipe (the flooding) was initiated in an annular flow state. In the range that U_{fL} was considerably low, i.e. the flooding velocity was as high as $U_G > 2$ m/s for $L_e = 60$ and 120 mm, the flooding occurred in a churn flow state where liquid and large bubbles were mixed up in a chaotic way. In the other cases, the flooding was brought about in a slug flow state where large gas plugs were observed in the liquid.

When U_{fL} and L_e are low, the flooding velocities are close to those of the open systems as shown in figures 5 and 6. However, flooding occurs generally at considerably lower gas velocities than those of the open systems. The higher the collapsed level L_e , the lower the flooding velocity. Then, as a matter of course, the relation between the flooding velocity U_G and the film flow rate U_{fL} shows a considerably different tendency from that of [2].

4. ANALYSIS ON BOTTOM-CLOSED SYSTEM FLOODING

4.1. Description of physical model

As described in the preceding section, the flooding of the bottom-closed system was caused generally by means that the liquid slug was pushed up by the air plug and reached the top of the test pipe, excluding the case of lower U_{fL} and L_e . Ueda & Koizumi (1993) examined the level swell

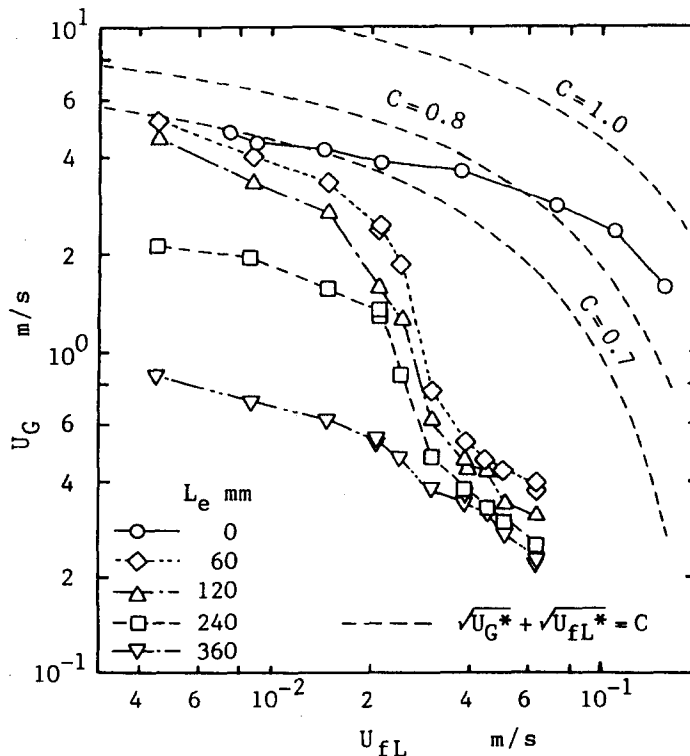


Figure 5. Flooding velocities of the bottom-closed system ($D = 26.0$ mm).

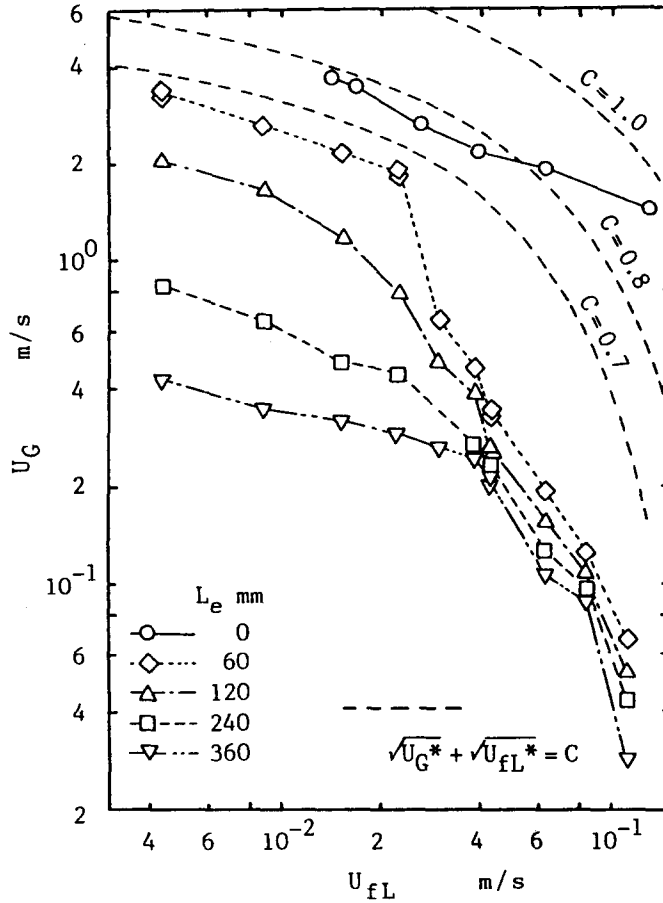


Figure 6. Flooding velocities of the bottom-closed system ($D = 14.8$ mm).

of the two-phase mixture in a pipe to which liquid was supplied as a falling film. It was supposed that the flooding studied here was associated with the behavior of the mixture level in such circumstances. Flooding of the bottom-closed system has been investigated based upon Ueda & Koizumi's analysis.

Employing the same apparatus that is illustrated in figure 2, Ueda & Koizumi measured the maximum and the minimum height; L_{max} and L_{min} , of the two-phase mixture level which swelled accompanying periodic fluctuations as the injected air flow rate was increased. Then, they derived the mean height of the mixture level $L_m = (L_{max} + L_{min})/2$ and its fluctuation amplitude $\Delta L = (L_{max} - L_{min})/2$ and analyzed these values. Their analysis was extended to flooding of the bottom-closed system as follows:

(1) *Mean mixture level height L_m .* When a flow state is of a slug type as illustrated in figure 7(a), the ratio of L_m to the water column height L_e is expressed with void fraction ϵ as

$$\frac{L_m}{L_e} = \frac{1}{1 - \epsilon} \tag{3}$$

The mean velocity of liquid between gas plugs is $U_G - U_{fL}$. Liquid falls down around the gas plug as the gas plug rises up, so that the cross-sectional velocity profile of the liquid between gas plugs may take such a form as that shown in figure 7(a). Assuming that the liquid velocity in the center portion of the pipe is $m_f U_G - U_{fL}$ and the gas plug has a relative velocity to this liquid velocity, the rise velocity of the gas plug can be expressed as (Nicklin *et al.* 1962)

$$u_G = m_f U_G - U_{fL} + c_s \sqrt{gD} \tag{4}$$

The term $c_s(gD)^{1/2}$ is the bubble rise velocity in stagnant liquid given by [1]. Since $\epsilon = U_G/u_G$, the following equation is derived from [3] and [4]:

$$\frac{L_m}{L_e} = \frac{m_f U_G - U_{fL} + c_s \sqrt{gD}}{(m_f - 1)U_G - U_{fL} + c_s \sqrt{gD}} \quad [5]$$

(2) *Level fluctuation amplitude ΔL* . It has been pointed out that the length of the liquid slug is stochastically distributed within a certain range (Akagawa *et al.* 1970). The variation of the liquid slug length is considered to result in the fluctuation of the mixture level around its mean height L_m given by [5].

Provided that the length of the liquid slug is within $h \pm \Delta h$, it is considered that the mixture level reaches the mean height L_m when the length of the liquid slug is equal to h , and reaches the maximum height L_{\max} when the length of the liquid slug is equal to $h + \Delta h$. The state where the top of the gas plug, which was associated with a liquid slug of $h + \Delta h$ on it, has just reached the elevation L_m is delineated in figure 7(b). Here the liquid slug of thickness Δh is still left on the gas plug.

Although the liquid ahead of the gas plug tip moves up at the same velocity that the gas plug has, the gas plug has a relative velocity $c_s(gD)^{1/2}$ to the liquid slug and a part of liquid in the slug falls down around the gas plug. Therefore, the liquid slug decreases its volume while it rises up further and is supplied with liquid by the film flow falling to it, and then reaches L_{\max} after Δt_0 to disappear ($\Delta h = 0$) eventually. The mass balance on the liquid slug during this period is given by

$$\frac{\pi D^2}{4} \Delta h + \frac{\pi D^2}{4} U_{fL} \Delta t_0 + \pi D \delta (\Delta L - \Delta h) - \frac{\pi D^2}{4} \epsilon_{pm} c_s \sqrt{gD} \cdot \Delta t_0 = 0, \quad [6]$$

where ϵ_{pm} is the mean void fraction of the gas plug and δ is the thickness of the falling film. The second term on the left-hand side of the equation represents the liquid supply due to the falling film flow, the third term represents the amount of liquid which exists as the falling film in the interval $(\Delta L - \Delta h)$ and the fourth term represents the volume of liquid which falls down around the gas plug.

By using Δt_0 obtained from [6], the rise height of the two-phase mixture level during this period is expressed as follows:

$$\Delta L = u_G \cdot \Delta t_0. \quad [7]$$

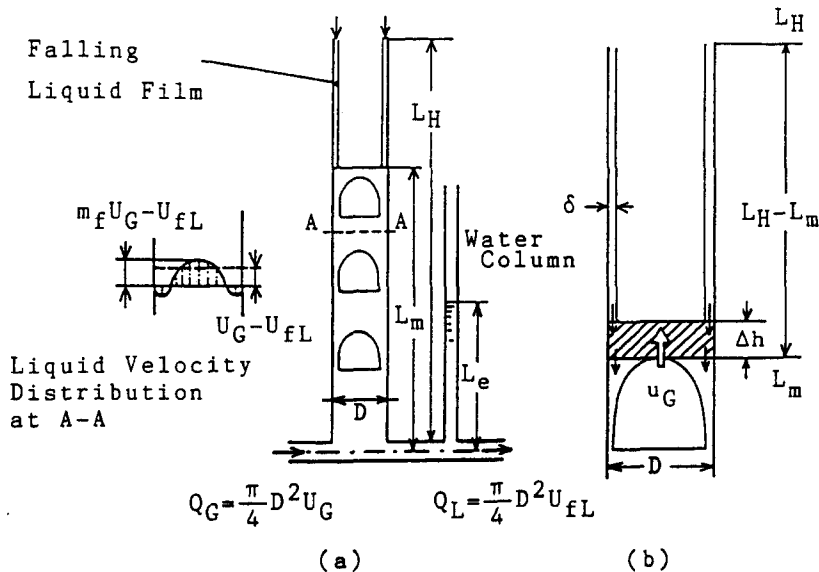


Figure 7. Flow state diagram of the two-phase mixture to which liquid is supplied as a falling film.

(3) *Onset of flooding.* Obviously from the above examination, the condition in which the maximum elevation of the two-phase mixture level $L_{\max} = L_m + \Delta L$ just reaches the pipe length L_H is regarded as the onset of flooding of the bottom-closed system. Thus, the incipient condition of flooding can be stated as

$$\frac{L_H}{L_e} - \frac{L_m}{L_e} = \frac{\Delta L}{L_e} \tag{8}$$

Substituting [5] and [7] into [8] with the aid of [4] and [6], and taking $\Delta L \gg \Delta h$, then

$$\frac{L_H}{L_e} - \frac{m_f U_G + c_s \sqrt{gD} - U_{fL}}{(m_f - 1)U_G + c_s \sqrt{gD} - U_{fL}} = \frac{\Delta h \cdot m_f}{L_e \cdot \epsilon_{pm}} \times \frac{U_G + \frac{c_s \sqrt{gD} - U_{fL}}{m_f}}{c_s \sqrt{gD} - \frac{U_{fL}}{\epsilon_{pm}} - \frac{4\delta}{\epsilon_{pm} D} (m_f U_G + c_s \sqrt{gD} - U_{fL})} \tag{9}$$

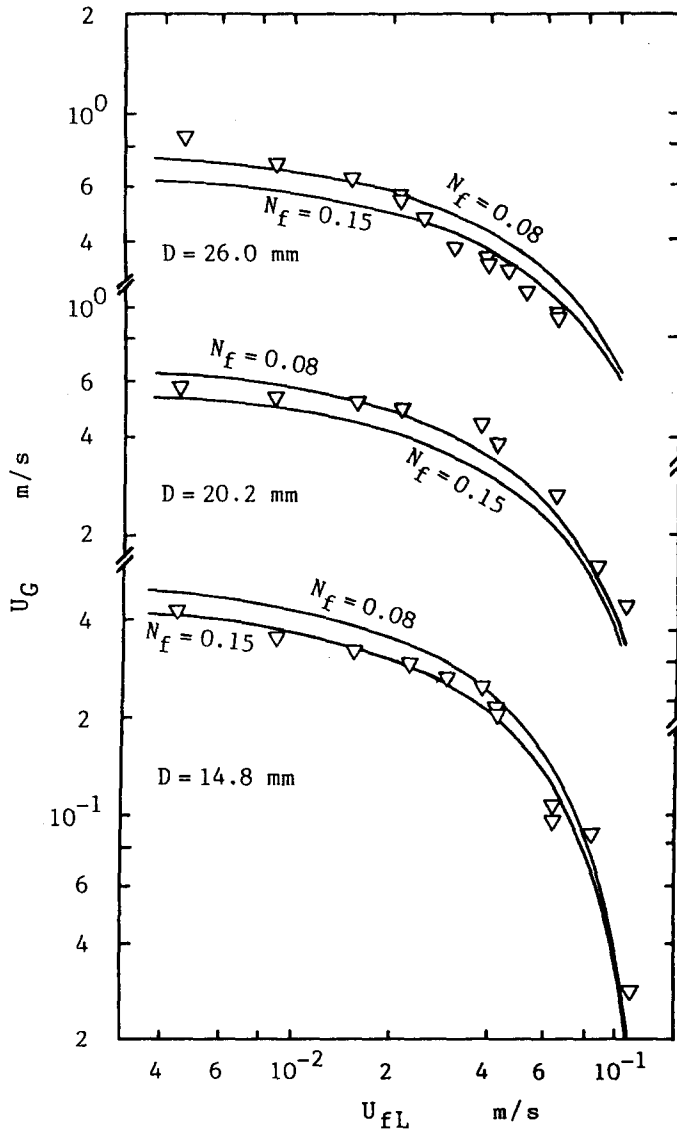


Figure 8. Comparison of measured and predicted flooding velocities of the bottom-closed system ($L_c = 360$ mm).

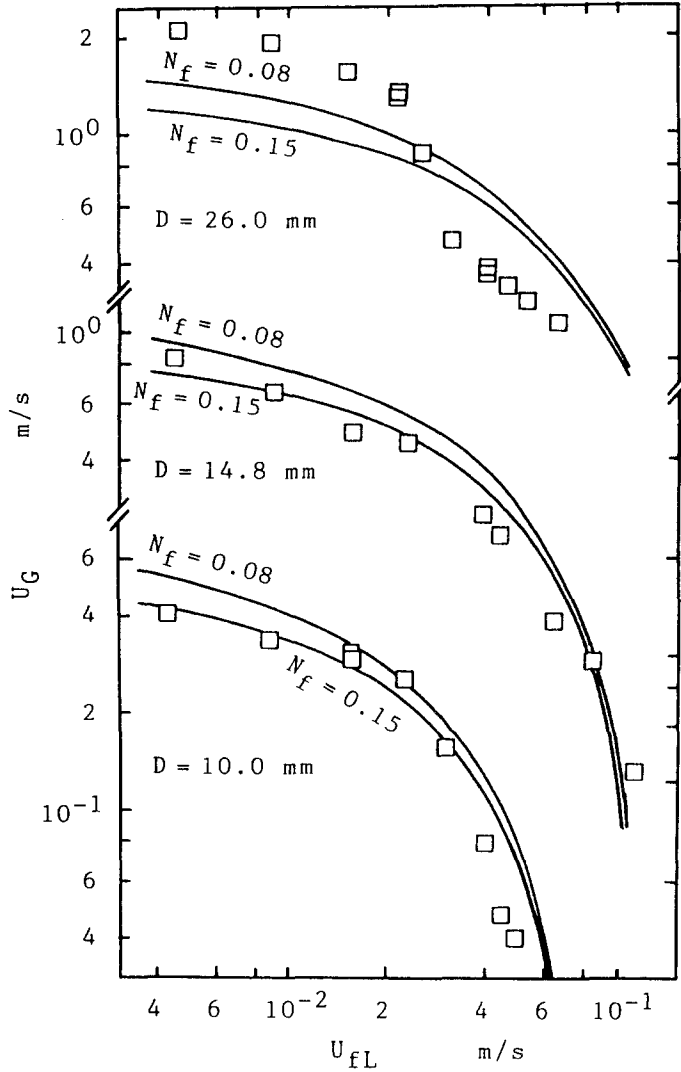


Figure 9. Comparison of measured and predicted flooding velocities of the bottom-closed system ($L_e = 240$ mm).

Since both ϵ_{pm} and m_f are close to unity, $U_G \gg U_{fL}$ and also $4\delta/D \ll 1$, the above equation can be approximated as follows:

$$\frac{L_H}{L_e} \frac{U_G + c_s \sqrt{gD} - U_{fL}}{(m_f - 1)U_G + c_s \sqrt{gD} - U_{fL}} = N_f \frac{U_G + c_s \sqrt{gD} - U_{fL}}{c_s \sqrt{gD} - U_{fL} - \frac{4\delta}{D} (U_G + c_s \sqrt{gD} - U_{fL})}, \quad [10]$$

where

$$N_f = \frac{\Delta h \cdot m_f}{L_e \cdot \epsilon_{pm}} \quad [11]$$

is a parameter for the fluctuation amplitude of the liquid slug length.

Therefore, the flooding velocity U_G of the bottom-closed system can be predicted from [10], by finding the value of U_G that satisfies [10] for a given U_{fL} . For m_f and N_f necessary in the calculation of [10], the following correlations have been proposed by Ueda & Koizumi (1993):

$$m_f = (1.175 \pm 0.075) - 1.15 \frac{U_{fL}}{c_s \sqrt{gD}} \left[\frac{D}{L_e} \right]^{1/2} \quad [12]$$

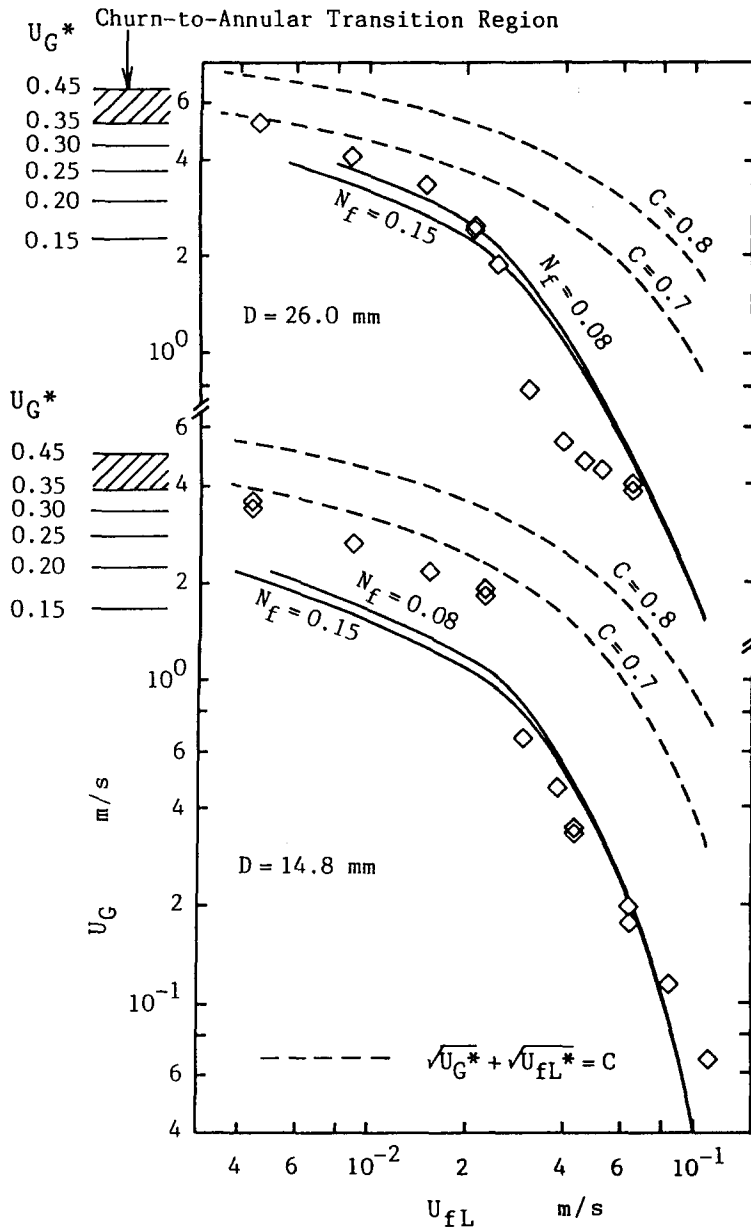


Figure 10. Comparison of measured and predicted flooding velocities of the bottom-closed system ($L_c = 60$ mm).

and

$$N_f = 0.08 \sim 0.15. \tag{13}$$

4.2. Comparison with experimental results

Flooding velocities of the bottom-closed system measured in the present experiments are compared with values predicted by [10] hereafter.

In the calculation, the falling film thickness δ was obtained with the Kapitza equation and the universal velocity profile equations (Ueda 1981) following Ueda & Koizumi (1993). These equations give the relations between δ and the film Reynolds number, as briefly introduced in the latter reference. Equation [12] was used for m_f , where the constant of the first term on the right-hand side was set to 1.10. Since flooding is defined as the initiation of splashing-out of the

liquid from the top of the pipe, the highest value of the mixture level rather than the mean of the maximum height is concerned with the onset of flooding. Thus, the lowest value of the constant in [12] was adopted which provides a higher value of L_m .

Predicted flooding velocities are compared with the measured values in figures 8 and 9, where L_e was high and flooding was initiated in a slug flow state. In the figures, the solid lines are the predicted with $N_f = 0.08$ and 0.15. Although the data for $D = 26.0$ mm in figure 9 are scattered, [10] reproduces most experimental results very well.

Figure 10 describes the comparison of measured and predicted flooding velocities for the case of low L_e . In the experiments, flooding was initiated in an annular or churn flow state at low U_{fL} , whereas at high U_{fL} it was initiated in a slug flow state. In the figure, flooding velocities of the open system calculated with [2] using $C = 0.7$ and 0.8 (refer to figure 4) are included for comparison. In the case where flooding occurred in an annular flow state, the measured flooding velocities are close to the values calculated with [2]. On the other hand, in the case where it occurred in a slug flow state, the measured values are close to the values calculated with [10].

Ueda & Koizumi (1993) suggested that when air was injected into a stagnant liquid column, transition of a flow state of the two-phase mixture to an annular type came out in the following range of non-dimensional superficial velocities of air:

$$U_G^* = \frac{U_G}{\sqrt{gD}} \left(\frac{\rho_G}{\rho_L - \rho_G} \right)^{1/2} = 0.35 \sim 0.45.$$

The shaded area in figure 10 indicates the region of the air velocities obtained from this relation. In the region of $U_G^* > 0.20$, the measured flooding velocities at low U_{fL} are a little higher than the values calculated with [10], and in the case of

$$U_G^* \geq 0.35, \quad [14]$$

the measured flooding velocities came up to values close to the open-system flooding velocities.

5. CONCLUSIONS

The initiation conditions of liquid splashing-out from the top of a pipe, i.e. the initiation of liquid ascent or flooding, were examined experimentally for both an open system, where only a falling film and an ascending gas flow exist in the pipe, and a bottom-closed system, where a liquid film flows down to the bubbling two-phase mixture in the lower portion of the pipe. The conclusions derived are as follows:

- (1) In the open system, the Wallis correlation for the flooding velocity provided adequate results when flooding occurred in an annular flow state.
- (2) In the bottom-closed system, when the superficial velocity of the falling film U_{fL} was small and the collapsed liquid level L_e in the pipe was low, flooding was initiated in an annular flow state. The flooding velocities in such a case were close to those of the open system.
- (3) However, as U_{fL} and/or L_e were increased, a flow state in the pipe changed to take a slug type and the swell of the fluctuating mixture level came to yield flooding. The flooding velocities were considerably lower than those of the open system and decreased with an increase in L_e .
- (4) For the bottom-closed system with a slug type mixture, the relation between the flow rates of the falling film and gas and the two-phase mixture level swell was analyzed physically and the correlation for predicting the flooding velocity was proposed. The correlation reproduced the experimental results well.

REFERENCES

- Akagawa, K., Hamaguchi, H. & Sakaguchi, T. 1970 Study on differential pressure fluctuation of two-phase slug flow (third report). *Trans. J. Soc. Mech. Engrs* **36**, 1535–1542.
- Nicklin, D. J., Wilkes, J. O. & Davidson, J. F. 1962 Two-phase flow in vertical flow. *Trans. Inst. Chem. Engrs* **40**, 61–68.

- Suzuki, S. & Ueda, T. 1977 Behavior of liquid films and flooding in counter-current two-phase flow—Part 1. Flow in circular tubes. *Int. J. Multiphase Flow* **3**, 517–532.
- Ueda, T. 1981 *Two-phase Flow and Heat Transfer*, pp. 85–89 and 128–132. Yokendo, Tokyo.
- Ueda, T. & Koizumi, Y. 1993 Two-phase mixture level swell in vertical pipes. *Int. J. Multiphase Flow* **19**, 1–13.
- Ueda, T. & Miyashita, T. 1991 On the performance limit of closed two-phase thermosiphons. *Heat Transfer Jap. Res.* **20**, 602–617.
- Wallis, G. B. 1969 *One-dimensional Two-phase Flow*, pp. 336–339, McGraw-Hill, New York.
- White, E. T. & Beardmore, R. H. 1962 The velocity of rise of single cylindrical air bubbles through liquids contained in vertical tubes. *Chem. Engng Sci.* **17**, 351–361.